Colloids and Surfaces A 546 (2018) 285–292

Contents lists available at ScienceDirect

Colloids and Surfaces A

journal homepage: www.elsevier.com/locate/colsurfa

Octyl *p*-methoxycinnamate loaded microemulsion based on *Ocimum basilicum* essential oil. Characterization and analytical studies for potential cosmetic applications

Verónica Volpe, Danielle Silva Nascimento, Matías Insausti, Marcos Grünhut*

INQUISUR (UNS-CONICET), Department of Chemistry, Universidad Nacional del Sur, 1253 Alem Avenue, B8000CPB, Bahía Blanca, Argentina

GRAPHICAL ABSTRACT

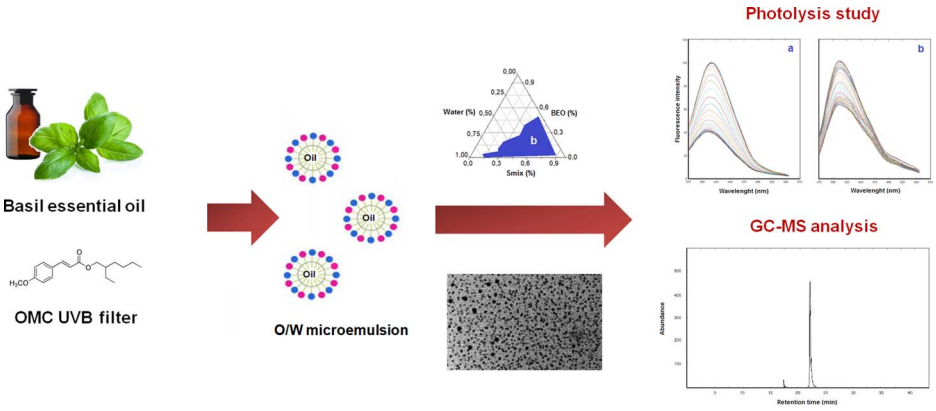

ARTICLE INFO

Keywords:
Microemulsion
Ocimum basilicum
Essential oil
Octyl *p*-methoxycinnamate
Photolysis study
Antiinflammatory activity
Mosquito repellent

ABSTRACT

A O/W microemulsion based on biocompatible materials was designed for a potential topical use as UVB filter, antiinflamatory and mosquito repellent. Octyl-p-methoxy cinnamate (OMC) is one of the most widely used sunscreen compounds. Nevertheless, their efficiency as UV filter is affected by irradiation because a photolysis process occurs. *Ocimum basilicum* essential oil is utilized in traditional medicine and as repellent of insects, among others. Hence, the proposed O/W microemulsion consisted of 6.0% of *Ocimum basilicum* essential oil (oil phase), 23% of a 2:1 mixture of decaethylene glycol mono-dodecyl ether (surfactant) and ethanol (co-surfactant), and 71% of water. OMC was successfully loaded in the O/W microemulsion (1.5%). The loaded system presented a particle size of (12.60 ± 0.10) nm and a polydispersity index of 0.389 ± 0.042. A spherical morphology and droplet sizes in nanometric range were corroborated by transmission electronic microscopy. The higher photostability of OMC in the O/W microemulsion with respect to the free-OMC was demonstrated by calculating the photolysis kinetic constants (0.00186 s^{-1} and 0.00457 s^{-1}, respectively) which were obtained through a photolysis study assisted by multivariate curve resolution-alternating least squares algorithm. Moreover, the stability of the system over time and under different conditions was demonstrated. On the other hand, a chromatographic analysis of the essential oil corroborated the presence of estragole (93.2%) which presents a documented antiinflammatory activity, and seven compounds with a well reported mosquito repellent

* Corresponding author.
E-mail address: mgrunhut@uns.edu.ar (M. Grünhut).

https://doi.org/10.1016/j.colsurfa.2018.02.070
Received 30 November 2017; Received in revised form 9 February 2018; Accepted 28 February 2018
Available online 02 March 2018
0927-7757/

activity, such as linalool (2.81%), cineole (0.57%), among others. On this form, the proposed O/W microemulsion presents optimal chemical and physicochemical characteristics for a potential application in cosmetic products.

1. Introduction

Several studies on photoprotection for human skin are of increasing importance because of the negative effects of exposure to solar radiation. It is well known that UV radiation causes sunburns, skin aging and after a long period of time, it may cause skin cancer [1]. Sunscreens are chemicals with the function of protecting the skin from the damaging effects of the sun. These molecules are usually organic compounds capable of absorbing UV or inorganic molecules which are able to block UV rays [2]. The octyl-*p*-methoxycinnamate (OMC) is an organic compound that protects against UV radiation. OMC is widely used in personal care products and represents one of the most common liposoluble absorbers incorporated in sunscreen formulations. OMC absorbs radiation in the wavelength region of 290–320 nm (UVB region) [3]. However, when OMC is exposed to sunlight, it is rendered less effectively, with a decrease in the UV absorption. This decrease of the efficiency of the OMC can be improved using appropriate vehicles as carriers of OMC. Thus, polymeric nanocapsules [4], lipid nanoparticles [5] and solid lipid nanoparticles [6] have been proposed as potential vehicles of OMC. Recently, Nascimento et al. proposed a new carrier for OMC based on a O/W microemulsion [7].

Microemulsions are systems formed by oil, water and surfactant, which are frequently combined with a cosurfactant, that can be classified as oil-in-water (o/w), water-in-oil (w/o) or bicontinuous systems depending on their structure. Physico-chemical properties of these systems include transparency, optical isotropy and thermodynamic stability with a droplet size usually in the range of 10–200 nm [8]. Because of the presence of both lipophilic and hydrophilic domains, microemulsions are appropriate systems to incorporate a wide range of molecules, such as pharmaceuticals and several compounds used in personal care products [9]. Microemulsions present advantages such as allowing the release of the substance which is encapsulated in a sustained manner and the ability to protect labile compounds against chemical degradation and photodegradation induced by UV radiation [10]. Besides, the typical components used for the preparation of microemulsions are usually good permeation enhancers. Thereby, microemulsions show a significant enhancement effect on transdermal delivery over the conventional formulations.

The incorporation of essential oils as the oil phase into vehicles such as microemulsions is an interesting feature because in addition to the improvement in the solubility and bioavailability of lipophilic compounds, they provided to the system their inherent properties [11]. In particular, *Ocimum basilicum* essential oils are used in traditional medicine as anti-inflammatory, antioxidant, antimicrobial, antifungal, larvicidal and repellent of insects [12]. These properties are based on the presence of bioactive and volatile compounds, such as estragole, linalool, cineol, α-terpineol, α-pinene, β-pinene, among others. The anti-inflammatory and antiedematogenic activity of the *Ocimum basilicum* essential oil was recently observed by means of an *in vivo* study [13]. Moreover, the mosquito repellent activity of this essential oil is well documented [14], including against *Aedes aegypty* [15]. This genus of mosquito is the main vector that transmits the viruses that cause diseases such as dengue, zika and chikungunya [16]. On the other hand, it is important to note that the *Ocimum basilicum* essential oil is a biocompatible component. Previous studies based on skin irritation test in rats have demonstrated that there was not any observable reaction with *Ocimum basilicum* essential oil [14].

In this work an *Ocimum basilicum* essential oil based O/W microemulsion as a vehicle for a chemical UVB filter (OMC) and with a potential use as anti-inflammatory and mosquito repellent is proposed. The system was physico-chemically characterized by means of dinamic light scattering (DLS) among other techniques. The morphology of the proposed O/W microemulsion was evaluated by transmission electronic microscopy (TEM). Additionally, a photolysis study was performed using a continuous flow system and monitored by molecular fluorescence spectroscopy. The spectral data were analyzed by multivariate curve resolution-alternating least squares (MCR-ALS) in order to obtain the kinetic rate constants associated to the photolysis of the OMC. Besides, the characterization of the *Ocimum basilicum* essential oil used was performed by gas chromatography-mass spectrometry (GC–MS) in order to evaluate the presence of components with both anti-inflammatory and mosquito repellent activity. Besides, a stability study of the system was carried out and *in vitro* method was used for solar protection factor determination.

2. Materials and methods

2.1. Materials

Decaethylene glycol mono-dodecyl ether (Sigma-Aldrich®) and ethyl alcohol (Dorwil®) were used as non-ionic surfactant and co-surfactant, respectively. *Ocimum basilicum* essential oil (Euma®) was used as oil phase and octyl-*p*-methoxy cinnamate (Parafarm®) was used as UVB filter. Ultra-pure water (18 MΩ cm^{-1}) was obtained from a Barnsted® water purification system.

2.2. Methods

2.2.1. Microemulsion components and phase behaviour

The microemulsions were prepared as carriers of OMC by considering three biocompatible materials: decaethylene glycol mono-dodecyl ether (DME), ethyl alcohol (ETA) and *Ocimum basilicum* essential oil (BEO). The relation of these components required for the preparation of microemulsions was obtained by means of pseudo-ternary phase diagrams. These diagrams were performed by varying the percentages of the aqueous phase, surfactant:co-surfactant mixture (DME:ETA) and oil using the aqueous titration method at room temperature (25 °C). The weight ratio of DME:ETA (S_{mix}) was varied as 1:2, 2:1 and 3:1. Thus, three pseudo-ternary phase diagrams were obtained. Then, for each phase diagram the corresponding S_{mix} was mixed with the oil at the weight ratios 0.5:9.5; 1:9; 2:8; 3:7; 4:6; 5:5; 7:3; 8:2 and 9:1, respectively. Each weight ratio mixture (S_{mix}:BEO) was then gradually titrated with ultra-pure water, under moderate magnetic stirring. The mixtures were visually examined and the microemulsion region was defined as transparent and isotropic mixtures. The rest of the diagram corresponded to phase alterations, where turbidity was observed.

2.2.2. Preparation of OMC loaded microemulsions

OMC loaded microemulsions were obtained by adding and stirring at 25 °C the OMC to the oil phase in order to obtain a final concentration of 1.0, 1.5 and 2.0% (w/w). These concentrations were chosen considering the permitted level in cosmectic products for both, Food and Drugs Administration (7.5%) and European Union (10%) [17]. Then, this mixture was added to the corresponding S_{mix} and titrated with ultra-pure water under moderate magnetic stirring. All the prepared OMC loaded microemulsions were stored in amber-glass containers at room temperature (25 °C).

2.2.3. Physico-chemical characterization of the microemulsions

The conductivity of the preparations at 25 °C was determined using

an Adwa® model AD32. An Atago® model RX-5000 refractometer was used for the determination of the refractive indices. The pH measurements were performed by using an Orion model 710 A pH meter with an Orion-Ross® model 81-02 electrode. 5.0 g of OMC loaded microemulsion was dispersed in 50 mL of ultra-pure water. The dispersion was stirred during 2 h at room temperature (25 °C). Average droplet size (Z) and polydispersity index (PdI) were determined by dynamic light scattering (DLS) using a Malvern Zetasizer Nano Series instrument. The measurements were performed at room temperature and at a 90° angle.

2.2.4. Morphology of the OMC loaded microemulsion

The morphology of the microemulsion was evaluated by transmission electronic microscopy (TEM) by using a JEOL 100 CXII transmission electron microscope operated at 80 kV. A drop of the microemulsion was placed onto a Formvar coated copper grid (200 mesh) and a negative staining with uranyl acetate solution was performed for 1 min. Previous to the observation, the sample was dried at room temperature.

2.2.5. Stability study of the OMC loaded microemulsion

The stability study of the OMC loaded microemulsion included a centrifugation test followed by a series of heating-cooling cycles. At first, the OMC loaded microemulsion was centrifuged at 3000 rpm for 30 min by using a Rolco® model CM 2036 centrifuge. Then, a total of three heating-cooling cycles per microemulsion were performed. Each cycle consisted of the storage of the OMC loaded microemulsion for 48 h at 4 °C followed by 48 h at 40 °C.

2.2.6. Characterization of the Ocimum basilicum essential oil

The characterization of the *Ocimum basilicum* essential oil used to obtain the proposed O/W microemulsion was carried out by gas chromatography–mass spectrometry (GC–MS). The analysis was performed by using an Agilent GC model 7890B gas chromatograph equipped with fused silica capillary HP-5 column (30 m × 0.25 mm i.d.; film thickness 0.25 μm) and coupled with 5977A mass spectrometer. The temperature of the injector was kept at 290 °C and helium was used as the carrier gas at a flow rate of 1.0 mL min^{-1}. The oven temperature program was 40–100 °C at the rate of 3 °C min^{-1} and then programmed to 280 °C at the rate of 10 °C min^{-1}. Finally, the oven temperature was kept at 280 °C for 5 min. The split ratio was 1:20. Ion source and interface temperatures were 230 and 260 °C, respectively. The mass range was 40–500 atomic mass units. The compounds were identified by comparing mass spectra in the computer libraries.

2.2.7. Photolysis study of the OMC loaded microemulsion

A comparative photolysis study between the OMC in aqueous medium and OMC loaded microemulsion was performed by a continuous flow system with molecular fluorescence detection coupled to a photoreactor (Fig. 1). Then, the spectral data were analyzed by MCR-ALS algorithm in order to obtain the kinetic rate constants corresponding to the photolysis process in both OMC-aqueous and OMC loaded microemulsion. The sample of OMC in aqueous medium was prepared in order to obtain a OMC final concentration of 1.5% (w/w). Due to the fact that OMC is a lipophilic molecule, 0.15 g of OMC were diluted in 10 mL of ethanol.

2.2.7.1. Photoreaction system. The photolysis study was performed using a lab-made UVB photoreactor coupled to a continuous flow system. Then, the photolysis process was monitored on line by molecular fluorescence (Fig. 1). The lab-made UVB photoreactor consisted of 12 m long of PTFE tube (0.5 mm i.d.) which was rolling helically around a Philips® low mercury UVB lamp (15 W). The samples were pumped to the photoreactor with a Gilson minipuls 3 peristaltic pump. When the photoreactor was filled, the UVB lamp was turned ON for 12 min. The flow rate was optimized in order to elute the loaded volume in the photoreactor (9.42 mL) in 12 min. Then, the samples coming from the photoreactor were towards a flow quartz cell (150 μL) used in right-angle geometry and located in a Jasco FP-6500 spectrofluorometer. The slit width was 3 nm for both, excitation and emission. The excitation wavelength was performed at 354 nm and the emission spectra were registered between 370 and 550 nm. The scan rate was 500 nm min^{-1} and the photomultiplier tube (PMT) voltage was 600 V. The acquisition interval and integration time was fixed at 0.1 nm and 1.0 s, respectively. So, fluorescence spectra were registered every 30 s, adding 24 spectra per sample. The emission signals were registered every 0.1 nm, so every spectra consisted of 1800 variables.

2.2.7.2. Data analysis. Considering the number of spectra per sample (24) and the number of variables per spectrum (1800) the data corresponding to each sample were arranged in a matrix of 24 × 1800. The data analysis was performed by MCR-ALS using MCR-ALS_GUI_2.0 toolbox [18] written in MatLab® environmental [19]. It is a known fact that, this algorithm consists of a mathematically decomposition of the analytical signal into the contributions due to the pure components in the system, which can be written as a bilinear model of pure component contributions, as follows:

$$\mathbf{D} = \mathbf{C}\mathbf{S}^{T} + \mathbf{E} \quad (1)$$

where **D** is the experimental fluorescent data matrix, **C** is the matrix describing the changes in the concentration of the species present in the system under study, $\mathbf{S}^T$ is the matrix containing the fluorescent spectra of these species, and **E** is the residual matrix with the data variance unexplained by $\mathbf{C}\mathbf{S}^T$. During the optimization, some constraints were applied, such as, non-negativity for both, spectra and concentration profiles. On the other hand, a constraint related to the proposed kinetic model was considered.

2.2.8. Solar protection factor of OMC loaded microemulsion

The *in vitro* Mansur method [20] was applied in order to obtain the solar protection factor (SPF) for the proposed OMC loaded microemulsion. For this purpose, the O/W microemulsion was diluted in

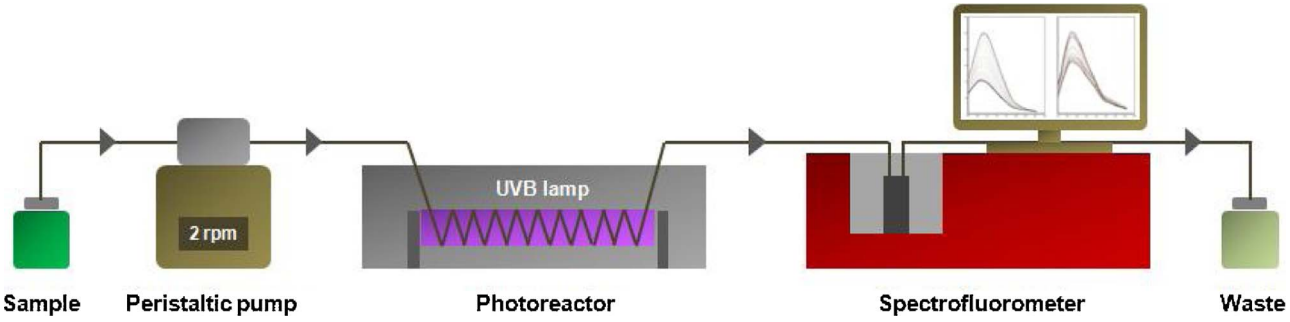

Fig. 1. Scheme of the continuous flow system used for the photolysis study. The arrows indicate the direction of the flow (0.78 mL min^{-1}).

ethanol at a final concentration of 0.2 mL mL^{-1}. Then, the spectrophotometric measurements each 5 nm between 290 and 320 nm were obtained by using a Hewllet Packard 8453 UV–vis spectrophotometer equipped with a quartz cell (10 mm optical path). The SPF was calculated as follows:

$$SPF = CF \sum_{290}^{320} EE_{(\lambda)} I_{(\lambda)} A_{(\lambda)} \quad (2)$$

where CF is a correction factor (in this case, 10), EE is the erythemal effect spectrum, I is the solar intensity spectrum and A is the measured absorbance of the OMC-ME at each wavelength. The relationship between the erythemal effect spectrum and the solar intensity spectrum at each wavelength (EE × I) was determined as described by Sayre et al. [21].

3. Results and discussion

3.1. Phase behavior

The phase diagrams allow to find out the concentration range of components to create microemulsions easily. The Fig. 2a–c shows the three pseudo-ternary phase diagrams corresponding to each weight ratio of DME:ETA (S_{mix}) tested, *i.e.* 1:2, 2:1 and 3:1, respectively. For each phase diagram, the microemulsion region is represented by the blue area and corresponding to clear and transparent mixtures. The rest of the region represents turbid emulsions in each case. In all cases, as the Smix concentration was increased, it was possible to add more BEO to the system, and thereby, to increase the final amount of BEO. On the other hand, the microemulsions with a 2:1 DME:ETA ratio exhibited the highest stability over time, with respect to the other systems tested and, therefore, this surfactant:co-surfactant ratio was selected for further studies (Fig. 2b).

3.2. Characterization of the O/W microemulsions

It is well known that microemulsions used as delivery vehicles of lipophilic molecules should be kept both surfactant and co-surfactant levels as low as possible. On the other hand, the *Ocimum basilicum* essential oil content has to be high enough to allow to load OMC at effective levels for their potential use as sunscreen and provide optimal activities as anti-inflammatory and repellent of insects. For this reason, six microemulsions containing between 6 and 10% of BEO were chosen. The composition of the selected microemulsions are shown in Table 1. Hence, ME1 to ME6 were loaded with 1.5% de OMC. This concentration was considered as optimal because appropriate Z and PdI values were obtained (S1).

Table 1
Composition of selected O/W microemulsions.

Sample	BEO*	OMC*	Smix*	Water*
ME1	6.0	–	23.0	71.0
ME2	8.0	–	32.0	60.0
ME3	8.5	–	34.0	57.5
ME4	9.0	–	36.0	56.0
ME5	9.5	–	35.0	55.5
ME6	10.0	–	40.0	50.0
OMC-ME1	6.0	1.5	29.0	63.5
OMC-ME2	6.5	1.5	32.0	60.0
OMC-ME3	7.0	1.5	34.0	57.5
OMC-ME4	7.5	1.5	36.0	56.0
OMC-ME5	8.0	1.5	35.0	55.5
OMC-ME6	8.5	1.5	40.0	50.0

* The concentrations are expressed in % (w/w).

Physico-chemical parameters such as, Z, PdI, pH, refractive index and conductivity were performed in both, OMC free (ME1 to ME6) and OMC loaded microemulsions (OMC-ME1 to OMC-ME6), and the results are shown in Table 2.

The conductivity of the analyzed microemulsions were in range 0.01–0.04 mS cm^{-1}, demonstrating that all the systems were O/W type. Moreover, the refractive index measurements were ranged between 1.36 and 1.39, indicating that the O/W microemulsions are isotropic systems. Regarding the pH, both OMC free and OMC loaded microemulsions presented appropiate values for topical use [22].

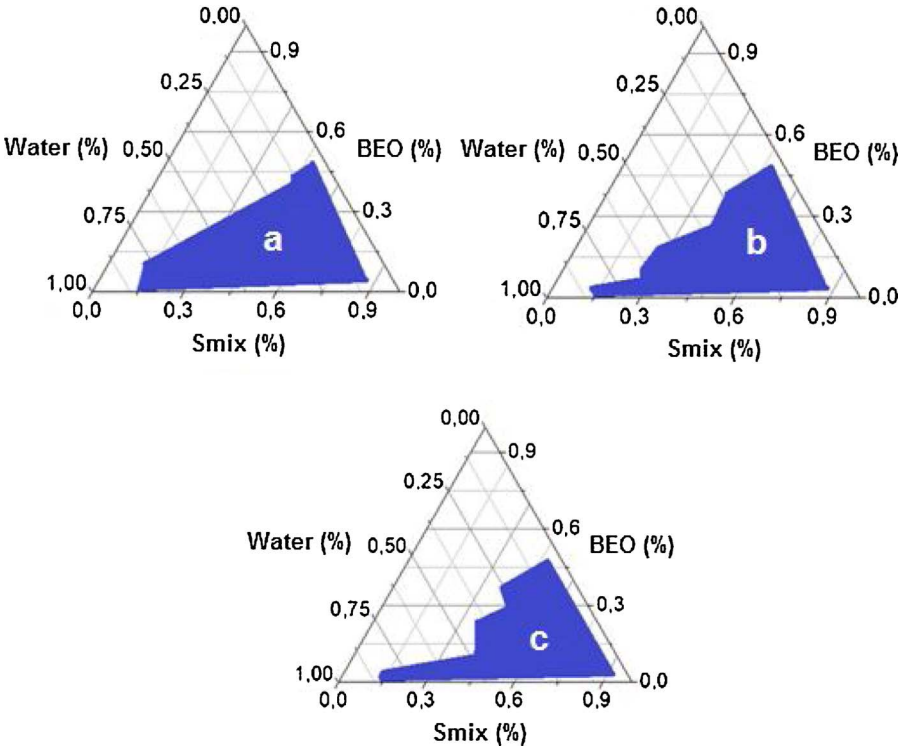

Fig. 2. Pseudo-ternary phase diagrams corresponding to the oil-surfactant:co-surfactant-water system at 25 °C. Smix correspond to a DME:ET ratio of 3:1 (a), 2:1 (b) and 1:1 (c).

Table 2
Physico-chemical characterization of the selected microemulsions.

Sample	Z (nm)	PdI	pH	RI	C (mS cm^{-1})
ME1	11.70 ± 0.10	0.228 ± 0.005	4.61 ± 0.03	1.36 ± 0.02	0.032 ± 0.002
ME2	12.90 ± 0.10	0.349 ± 0.003	4.93 ± 0.05	1.38 ± 0.02	0.041 ± 0.002
ME3	13.00 ± 0.30	0.395 ± 0.023	4.74 ± 0.03	1.38 ± 0.03	0.013 ± 0.003
ME4	13.40 ± 0.50	0.395 ± 0.017	4.73 ± 0.06	1.39 ± 0.02	0.029 ± 0.003
ME5	13.60 ± 0.20	0.390 ± 0.013	4.80 ± 0.07	1.39 ± 0.01	0.034 ± 0.001
ME6	12.40 ± 0.60	0.372 ± 0.010	5.00 ± 0.08	1.39 ± 0.02	0.030 ± 0.003
OMC-ME1	12.60 ± 0.10	0.389 ± 0.042	4.91 ± 0.03	1.37 ± 0.01	0.045 ± 0.003
OMC-ME2	15.20 ± 0.20	0.420 ± 0.010	4.70 ± 0.03	1.38 ± 0.01	0.028 ± 0.002
OMC-ME3	13.70 ± 0.20	0.523 ± 0.070	5.14 ± 0.05	1.38 ± 0.02	0.019 ± 0.001
OMC-ME4	14.50 ± 0.01	0.527 ± 0.081	4.81 ± 0.01	1.39 ± 0.03	0.033 ± 0.002
OMC-ME5	19.71 ± 0.41	0.619 ± 0.052	4.75 ± 0.10	1.39 ± 0.02	0.009 ± 0.002
OMC-ME6	23.27 ± 0.63	0.703 ± 0.046	4.77 ± 0.05	1.39 ± 0.02	0.011 ± 0.002

On the other hand, PdI represents the ratio of standard deviation to mean droplet size and varies from 0 to 1. A PdI value close to zero indicates a homogeneous system. A PdI between 0.2 and 0.4 indicates a narrow size distribution of the globule size approaching to a monodisperse system. As can be seen, the Z value for OMC free microemulsion was similar, varying between 11.69 and 13.59 nm. In all cases, the PdI varied between 0.228 and 0.395, demonstrating that the studied systems were monodispersive. Instead, for OMC loaded microemulsions, OMC-ME5 and OMC-ME6 presented higher Z values and were highly polydispersed systems (PdI: 0.619 and 0.703, respectively). However, for OMC-ME1 to OMC-ME4, although the Z values were similar, the PdI slightly increased from 0.388 to 0.527. Hence, based on the results mentioned before, the OMC-ME1 was selected as appropiate for further studies. Although OMC-ME1 contains a 6% of *Ocimum basilicum* essential oil, this microemulsion presented optimal physicochemical parameters as can be seen in Table 2.

3.3. Morphology of the OMC loaded microemulsion

In order to corroborate the droplet size and analyze the morphology of the droplets in the selected OMC loaded microemulsion (OMC-ME1), a TEM study was performed and the obtained photos are shown in Fig. 3. As can be seen, the selected microemulsion presented a spherical morphology and a droplet size in a nanometric range according to the previous results obtained by DLS technique.

3.4. Stability study of the OMC loaded microemulsion

OMC loaded microemulsion demonstrated no changes in physicochemical and general appearance such as clarity and transparency during the present study. No phase separation occurred after centrifugation test showing that the OMC-ME1 was physically stable. Besides, Z and PdI values were 12.34 nm and 0.359, respectively. Thus, as can be seen, these values did not change significatively after storing under studied conditions. This suggests that the OMC loaded microemulsion could remain stable in situations that involve environmental changes, such as storage, transport or distribution of the product.

3.5. Analysis of the Ocimum basilicum essential oil

Essential oils are complex mixtures of volatile organic compounds that are generated as secondary metabolites in plants. These mixtures are composed of hydrocarbons such as terpenes and oxygenated compounds such as alcohols, esters, ethers, aldehydes, ketones, lactones, phenols and phenol ethers [23]. The properties of the *Ocimum basilicum* essential oil such as antiinflammatory and repellent of insects are based on the presence of various of these bioactive and volatile compounds [13,24]. Therefore, a GC–MS analysis of the used *Ocimum basilicum* essential oil was performed and the results are shown in the Table 3. As can be seen, fifteen compounds (97.79% of the total composition) were separated and identified. The main component of the essential oil was estragole (1-methoxy-4-prop-2-enylbenzene), which was presented in a 93.2%. Estragole is a phenylpropanoid that presents well known anti-inflammatory properties [25]. The inflammation process is a defense mechanism characterized by pain, edema and infiltration of leukocytes to some external aggression, such as sunburns due to the UVB radiation exposure [26]. Recently, Rodrigues et al. [13] verified the anti-inflammatory properties of *Ocimum basilicum* essential oil with a high content of estragole in its chemical composition (60.9%). The anti-inflammatory action was verified using acute and chronic *in vivo* tests as paw edema, peritonitis, and vascular permeability and granulomatous inflammation model. The anti-inflammatory mechanism of action was analyzed by the participation of histamine and arachidonic acid pathways. The authors concluded that the reduction of both acute and chronic systemic inflammation occurs by the inhibition of mechanisms such as inhibition of receptors of chemical mediators, the metabolism of them and the migration of cells to the stimulated zone.

3.6. Photolysis study

The aim of this study was to compare the kinetic of the photolysis process of the OMC in an aqueous medium (OMC-aqueous) respect to

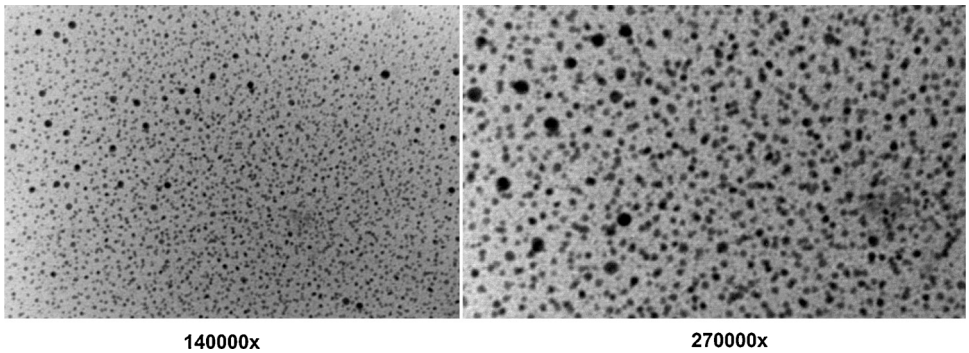

Fig. 3. TEM images of the selected OMC-ME1.

Table 3
GC–MS analysis of the *Ocimum basilicum* essential oil.

Compound	Activity	RT	MW	Formula	%
α-pinene	**IR**	**10.59**	**136.12**	**$C_{10}H_{16}$**	**0.03**
β-pinene	**IR**	**12.46**	**136.12**	**$C_{10}H_{16}$**	**0.05**
Cineole	**IR**	**15.00**	**154.14**	**$C_{10}H_{18}O$**	**0.57**
cis-oxide linalool		17.45	170.13	$C_{10}H_{18}O_2$	0.04
Linalool	**IR**	**18.38**	**154.14**	**$C_{10}H_{18}O$**	**2.81**
L-menthol		21.77	156.15	$C_{10}H_{20}O$	0.07
Ursodiol		21.91	392.29	$C_{24}H_{10}O_4$	0.04
Carveol		22.05	152.12	$C_{10}H_{16}O$	0.10
α-terpineol	**IR**	**22.44**	**154.14**	**$C_{10}H_{18}O$**	**0.17**
Estragole	**AI** [26]	**22.77**	**148.09**	**$C_{10}H_{12}O$**	**93.2**
Bornyl acetate	**IR**	25.07	196.15	$C_{24}H_{20}O_2$	**0.06**
Aromadendrene		26.89	204.19	$C_{15}H_{24}$	0.02
α-bergamotene		27.87	204.19	$C_{15}H_{24}$	0.35
β-caryophyllene	**IR**	**28.64**	**204.19**	**$C_{15}H_{24}$**	**0.02**
T-cadinol		30.77	222.19	$C_{15}H_{26}O$	0.26
Subtotal IR activity					**3.65**
Subtotal AI activity					**93.2**
Total					**97.79**

AI: Antiinflammatory; **IR**: insect repellent; **MW**: molecular weight; **RT**: retention time.

the OMC loaded in the proposed O/W microemulsion (OMC loaded microemulsion) in order to demonstrate the potential advantages of the OMC when it was loaded in the proposed O/W microemulsion. It is important to highlight that the direct photolysis of the OMC in an aqueous medium produces their photoisomerization, as follows:

Both E and Z isomers present a similar absorption wavelength. However, the molar absorption coefficient of the Z isomer is considerably lower than E isomer, resulting in a decreasing of the efficiency of the OMC as UV filter [27]. On the other hand, due to the fact that the E-OMC and the Z-OMC are fluorescent molecules, the photoisomerization process can be monitored by molecular fluorescence. Both species presented a maximum of excitation at 354 nm. Nevertheless, the maximum emission wavelength for E-OMC was 410 nm and for Z-OMC was 405 nm, which indicates a shift of the maximum emission wavelength for E-OMC during the photoisomerization process. On this form, the fluorescence spectra of OMC-aqueous and OMC loaded microemulsion were registered as a function of irradiation time by using the continuous flow system described in Section 2.2.7.1 (Fig. 1). In addition, the spectral behavior of the aqueous and O/W microemulsion media was studied. Fig. 4a and b shows the spectra corresponding to OMC-aqueous and OMC loaded microemulsion, respectively. In both cases, a decrease in the fluorescence signal intensity between 370 y 490 nm was observed over time. However, a visual approach demostrates that the photoisomerization of E-OMC to Z-OMC occurs faster in OMC-aqueous than OMC loaded microemulsion. The kinetic rate constants corresponding to OMC-aqueous and OMC loaded microemulsion were calculated by using the respective concentration profiles (Fig. 5). These profiles were obtained after the application of the MCR-ALS algorithm to the fluorescent spectral data. Thereby, the calculated kinetic rate constants k were 0.00457 s^{-1} and 0.00186 s^{-1} for OMC-aqueous and OMC loaded microemulsion, respectively. As can be seen, these values showed a

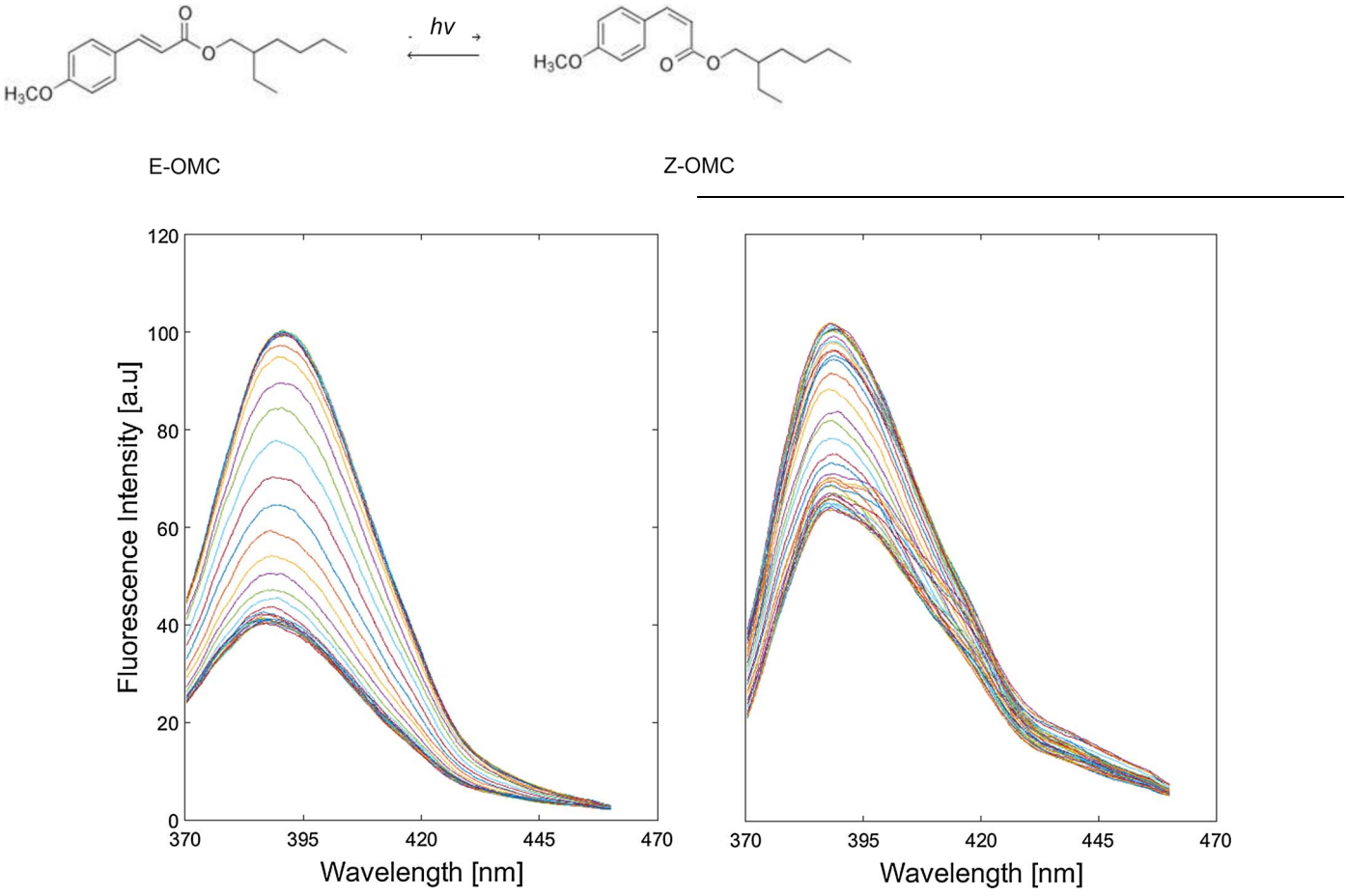

Fig. 4. Fluorescence spectra as a function of the irradiation time (12 min). The spectra correspond to the photolysis of the OMC in an aqueous medium (a) and the OMC loaded in the proposed O/W microemulsion (b).

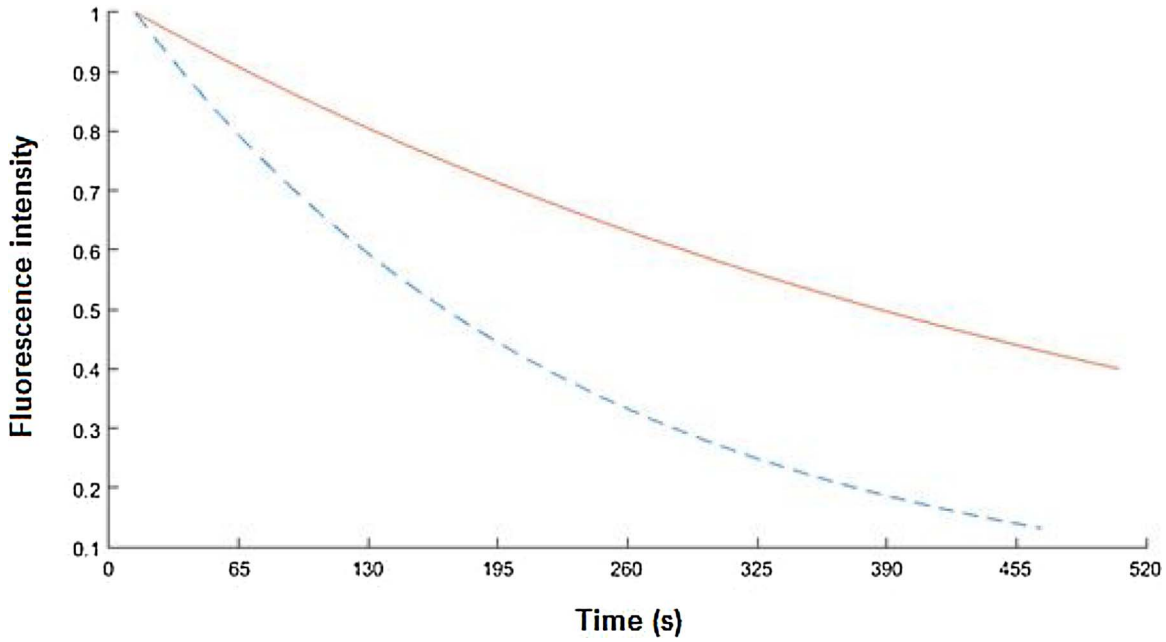

Fig. 5. Pure concentration profiles corresponding to the photolysis of the OMC. The blue and dotted line correspond to the OMC in an aqueous medium and the red line correspond to the OMC loaded in the proposed O/W microemulsion.

higher photoisomerization rate for OMC-aqueous than for OMC loaded microemulsion. This fact indicates that the proposed O/W microemulsion decreases the rate of the OMC photoisomerization induced by the UVB radiation, under the studied conditions. Both kinetic models were well explained with 98.6% and 99.3% of the explained variance, respectively.

3.7. Solar protection factor determination

The efficacy of the proposed system as solar protector was evaluated by means of the SPF determination. This factor can be defined as the relation between the UV energy required to produce a minimal erythema dose (MED) on protected skin and the UV energy required to produce a MED on unprotected skin (SPF = MED in sunscreen-protected skin/MED in non-sunscreen-protected skin). MED is the lowest time interval or dosage of UV radiation enough to produce a minimal and perceptible erythema on unprotected skin [28]. While higher the SPF is more effective the sunscreen is in preventing sunburns. Mansur et al. described an *in vitro* method to the determination of the SPF (section 2.2.8) [20], which presents an optimal correlation with *in vivo* studios [29]. The SPF obtained by the Mansur et al. method was 2.87. This value indicates that the proposed OMC loaded microemulsion increased almost three times the time to produce an erythema on skin in a person exposed to a low level of UVB radiation.

Moreover, the SPF was determined at different times of irradiation (3, 6, 9 and 12 min) in order to evaluate the efficacy of the OMC loaded microemulsion exposed to the UVB radiation. As can be seen in Fig. 6, in the first minutes there is a decrease of the SPF along the irradiation time. This fact is due to the lower molar absorption coefficient of the formed Z-OMC photoisomer with respect to the original E-OMC isomer. After this, the SPF was mantained constant, with a value around of 2. Beyond the fact that the performance the proposed OMC loaded microemulsion can be considered as optimal because of the formulation was loaded with an unique sunscreen, in comparison to commercial products that contain several UV filters (S2).

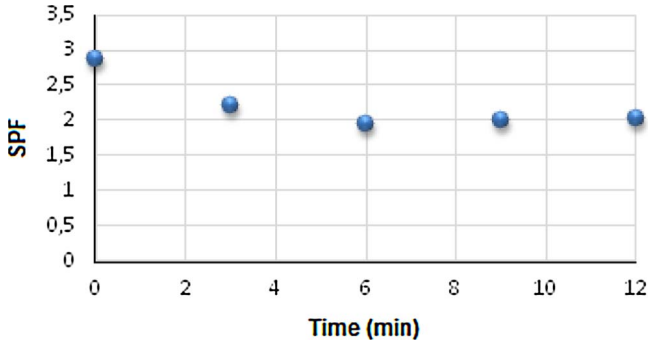

Fig. 6. SPF of the OMC loaded microemulsion over photolysis time (12 min).

4. Conclusions

This work demonstrates that the proposed O/W microemulsion based on an essential oil could be an effective vehicle for OMC chemical UVB filter. The system consisted of acceptable, biocompatible and accessible materials for topical use, such as, ethanol, decaethylene glycol mono-dodecyl ether, water and *Ocimum basilicum* essential oil.

The OMC loaded microemulsion was properly characterized and its morphology was analyzed. Moreover, the stability of the system over time and under different conditions was demonstrated. On the other hand, the photostability to the UVB radiation of the OMC loaded microemulsion was tested by means of an on-line photolysis system. Kinetic rate constants were obtained by the application of the MCR-ALS algorithm to the spectrofluorimetric data. This study showed that the photoisomerization of the OMC was slower when it was present in the O/W microemulsion with respect to the OMC in an aqueous medium. Besides, an *in vitro* based method allowed to calculate the solar protection factor, which was optimal for this kind of formulation.

A point to highlight is that the incorporation of *Ocimum basilicum* essential oil as oil phase to the system allows their use as anti-inflammatory and mosquito repellent. This fact is based on the presence of molecules with that activity in the essential oil, such as estragol, cineol and linanool, among others. This represents an interesting feature because an unique system could be able to reduce some consequences related to outdoors activities, such as sunburns, skin inflamation after solar exposition and mosquito bites. In short, these advantages could give added value to the cosmetic product. Besides,

this essential oil is a biocompatible component, it is easily adquirible due to the fact that it is used in traditional medicine and presents a relatively low cost.

Acknowledgments

The authors gratefully acknowledge the financial support from Consejo Nacional de Investigaciones Científicas y Técnicas (CONICET; PIP 11220120100625) and Universidad Nacional del Sur (PGI 24Q054).

Appendix A. Supplementary data

Supplementary material related to this article can be found, in the online version, at doi:https://doi.org/10.1016/j.colsurfa.2018.02.070.

References

[1] A.R. Abid, B. Marciniak, T. Pędziński, M. Shahid, Photo-stability and photo-sensitizing characterization of selected sunscreens' ingredients, J. Photochem. Photobiol. A 332 (2017) 241–250.
[2] P.G. Francis, M. Mitchnick, N.J. Frank, A review of sunscreen safety and efficacy, Photochem. Photobiol. 68 (1998) 243–256.
[3] S. Pattanaargson, T. Munhapol, P. Hirunsupachot, P. Luangthongaram, Photoisomerization of octylmethoxycinnamate, J. Photochem. Photobiol. A 161 (2004) 269–274.
[4] B.I. Olvera-Martínez, J. Cázares-Delgadillo, S.B. Calderilla-Fajardo, R. Villalobos-García, A. Ganem-Quintanar, D. Quintanar-Guerrero, Preparation of polymeric nanocapsules containing octylmethoxycinnamate by the emulsification-diffusion technique: penetration across the stratum corneum, J. Pharm. Sci. 94 (2005) 1552–1559.
[5] C. Puglia, F. Bonina, L. Rizza, P. Blasi, A. Schoubben, R. Perrotta, M.S. Tarico, E. Damiani, Lipid nanoparticles as carrier for octyl-methoxycinnamate: *in vitro* percutaneous absorption and photostability studies, J. Pharm. Sci. 101 (2012) 301–311.
[6] S.A. Wissing, R.H. Müller, The influence of solid lipid nanoparticles on skin hydration and viscoelasticity-*in vivo* study, Eur. J. Pharm. Biopharm. 56 (2003) 67–72.
[7] D. Silva Nascimento, M. Insausti, B.S. Fernández Band, M. Grünhut, Photolysis study of octyl p-methoxycinnamate loaded microemulsion by molecular fluorescence and chemometric approach, Spectrochim. Acta A Mol. Biomol. Spectrosc. 191 (2018) 277–282.
[8] M. Fanun, Microemulsionsas delivery systems, Curr. Opin. Colloid Interface Sci. 17 (2012) 306–313.
[9] P. Boonme, Applications of microemulsions in cosmetics, J. Cosmet. Dermatol. 6 (2007) 223–228.
[10] S. Songkro, N.L. Lo, N. Tanmanee, D. Maneenuan, P. Boonme, *In vitro* release, skin permeation and retention of benzophenone-3 from microemulsions (o/w and w/o), J. Drug Del. Sci. Technol. 24 (2014) 703–711.
[11] W. Treesuwan, M.A. Neves, K. Uemura, M. Nakajima, I. Kobayashi, Preparation characteristics of monodisperse oil-in-water emulsions by microchannel emulsification using different essential oils, LWT-Food Sci. Technol. 84 (2017) 617–625.
[12] S. Kale, A. Sonawane, A. Ansari, P. Ghoge, A. Waje, Formulation and *in vitro* determination of sun protection factor of Ocimum Basilicum, Linn. Leaf Oils Sunscreen Cream. Int. J. Pharm. Pharm. Sci. 2 (2010) 147–149.
[13] L.B. Rodrigues, A.O. Martins, F.R. Cesario, F.F. Castro, T.R. Albuquerque, M.N. Fernandes, B.A. Silva, L.J. Quintans Jr., J.G. Costa, H.D. Coutinho, R. Barbosa, I.R. Menezes, Anti-inflammatory and antiedematogenic activity of the *Ocimum basilicum* essential oil and its main compound estragole: *in vivo* mouse models, Chem. Biol. Interact. 257 (2016) 14–25.
[14] G. Baba, A.O. Lawal, H.B. Shariff, Mosquito repellent activity and phytochemical characterization of essential oils from *Striga hermonthica, Hyptis spicigera* and *Ocimum basilicum* leaf extracts, Br. J. Pharmacol. Toxicol. 3 (2012) 43–48.
[15] O. Chokechaijaroenporn, N. Bunyapraphatsara, S. Kongchuensin, Mosquito repellent activities of Ocimum volatile oils, Phytomedicine 1 (1994) 135–139.
[16] J. Patterson, M. Sammon, M. Garg, Dengue, zika and chikungunya: Emerging arboviruses in the new world, West J. Emerg. Med. 6 (2016) 671–679.
[17] R. Jansen, U. Osterwalder, S.Q. Wang, M. Burnett, H.W. Lim, Photoprotection: part II. sunscreen: development, efficacy, and controversies, J. Am. Acad. Dermatol. 69 (2013) 867.e1–867.e14.
[18] Multivariate Curve Resolution Homepage, http://www.mcrals.info.
[19] MATLAB®, The Mathworks, Inc., Natick, MA, USA.
[20] J.S. Mansur, M.N. Breder, M.C. Mansur, R.D. Azulay, Determination of sun protection factor by spectrophotometry, An. Bras. Dermatol. 61 (1986) 121–124.
[21] R.M. Sayre, P.P. Agin, G.J. Levee, E. Marlowe, A comparison of *in vivo* and *in vitro* testing of sunscreening formulas, Photochem. Photobiol. 29 (1979) 559–566.
[22] A.A. Badawi, A.B. El-Aziz, M.M. Amin, N.M. Sheta, Topical benzophenone-3 microemulsion based gels: preparation, evaluation and determination of microbiological UV blocking activity, Int. J. Pharm. Pharm. Sci. 6 (2014) 562–570.
[23] E. Guenther, The Essential Oils, Krieger Publishing Company, Florida, USA, 1972.
[24] L.S. Nerio, J. Olivero-Verbel, E. Stashenko, Repellent activity of essential oils: a review, Bioresour. Technol. 101 (2010) 372–378.
[25] F.M. Silva-Comar, L.A. Wiirzler, S.E. Silva-Filho, R. Kummer, R.B. Pedroso, R.A. Spironello, E.L. Silva, C.A. Bersani-Amado, R.K. Cuman, Effect of estragole on leukocyte behavior and phagocytic activity of macrophages, Evid.-Based Compl. Altern. Med. 2014 (2014) 1–7.
[26] M.A. Silva, G. Trevisan, C. Hoffmeister, M.F. Rossato, A.A. Boligon, C.I. Walker, J.Z. Klafke, S.M. Oliveira, C.R. Silva, M.L. Athayde, J. Ferreira, Anti-inflammatory and antioxidant effects of *Aloe saponaria* Haw in a model of UVB-induced paw sunburn in rats, J. Photochem. Photobiol. B 133 (2014) 47–54.
[27] K.M. Hanson, S. Narayanan, V.M. Nichols, C.J. Bardeen, Photochemical degradation of the UV filter octyl methoxycinnamate in solution and in aggregates, Photochem. Photobiol. Sci. 14 (2015) 1607–1616.
[28] R. Wolf, D. Wolf, P. Morganti, V. Ruocco, Sunscreens, Clin. Dermatol. 19 (2001) 452–459.
[29] E.A. Dutra, D.A. Oliveira, E.R. Hackmann, M.I. Santoro, Determination of sun protection factor (SPF) of sunscreens by ultraviolet spectrophotometry, Braz. J. Pharm. Sci. 40 (2004) 381–385.